WHITE LIGHT SKIN FRICTION AND GAS DENSITY MEASUREMENTS AROUND SUPERSONIC FOREBODY

Jean-Michel Desse*, Paulo d'Espiney**
***Office National d'Etudes et de Recherches Aérospatiales (ONERA), DAAP/MMHD, Centre de Lille, 5, Boulevard Paul Painlevé, 59045 Lille Cedex, France**
****Office National d'Etudes et de Recherches Aérospatiales (ONERA), DAAP/MHL, Centre de Châtillon, BP 72, Avenue de la Division Leclerc, 92322 Châtillon, France**

Keywords: Differential interferometry, Gas density field, Skin friction

Abstract

To quantify the aero-optical distortions of images recorded by optronic devices, models have to developed and validated by experiments. In that context, two types of experiments were performed at Mach 3.7 with a very high Reynolds number in the S3MA wind tunnel of ONERA. The first one concerns the measurement of the gas density field by differential interferometry using two large field Wollaston prisms and a polarized white light source. High speed interferograms are recorded at a framing rate of 20,000 pictures per second. Gas density profiles deduced assuming the flow to be axisymmetric show a good agreement with the results yielded by RANS computations. The second experiment concerns the oil-film interferometry skin-friction measurement under white light. The film height and variation over time have been measured by analyzing the fringes color. This one shows that very high accuracy can be achieved for interferograms analysis using a numerical model of the phenomenon based on a non constant stress assumption. The analysis of fringes color shows that a good agreement is obtained with RANS computations when the transition is imposed.

1 Introduction

Images recorded by optronic devices aboard supersonic profiles are very often disturbed by the aero-optical distortions induced by the shock wave generated around the profile and the boundary layer developing along the profile. In that context, aero-optical models need to be validated by experiments to quantify optical wavefront degradations for a better understanding of the underlying physics of the perturbating phenomena.

Therefore, two types of experiments were performed at Mach 3.7 with a very high Reynolds number in the S3MA wind tunnel of ONERA. The first one concerns the measurement of the gas density field through an optical bench based on differential interferometry using two large field Wollaston prisms and a polarized white light source. The existing coaxial optical setup working for the schlieren or shadowgraph visualizations has been adapted to the technique of differential interferometry. In this case, gas density variations in the test section produce variations in refractive index which change the interferogram colors. By analyzing the different tints of interferogram, the radial distribution of the optical path difference has been determined and gas density profiles have been deduced assuming the flow to be axisymmetric.

The second experiment concerns the oil-film interferometry skin-friction measurement under white light. The interference fringes obtained under white light by a thin oil film have been used to measure distribution of the skin-friction coefficient on a small window implemented in the ogive profile (lower surface). The film height and variation over time have been measured by analyzing the fringes color that is similar to those of Newton's scale. The use of color shows that very high accuracy can be achieved for interferograms analysis using a numerical model of the

phenomenon based on a non constant stress assumption.

The results of RANS calculations performed with the elsA software developed at ONERA were compared with the experimental data. A good agreement is obtained in terms of density profiles and skin friction when the transition is triggered from the ogive nose.

2. Gas density measurements

2.1 Experimental setup in ONERA S3MA wind tunnel

Differential interferometry using two Wollaston prisms and polarized white light has been implemented in the very large wind tunnel of ONERA S3MA. The principle of this technique is discussed in details by Gontier [1]. Briefly, a Wollaston prism decomposes a light vibration polarized in a given direction into two orthogonal vibrations of approximately equal amplitudes separated by a small birefringence angle. The two coherent rays cross the test section in different locations of the phenomenon so that the optical path difference becomes different for each ray. A second Wollaston prism and an analyzer are used to recombine the two rays and quantify the optical path difference. As a white light source is used, optical path differences produce color variations in the interferogram.

The existing schlieren coaxial optical setup has been modified for working in differential interferometry as it can be seen in Fig.1. The optical bench uses a xenon 150W white light source and it is equipped with two parabolic mirrors 800 mm in diameter, 20 m apart. Each prism is installed head to foot at the focal length of the parabolic mirrors. The Wollaston prisms are pasted with an angle α which fixes the birefringence angle and the sensitivity of the optical method. In order to visualize the phenomenon with two different sensitivities, two pairs of Wollaston prisms have been manufactured (α=0.5° and 2°), the distance between the two interfering rays being respectively 0.674 mm and 2.7 mm in the test section. As the field of view is very large (800 mm), specific Wollaston prisms have been manufactured following the recommendations of Françon [2]. In this manner, hyperbolic fringes observed in the field with classical prisms are carried on outside the field of view.

The schematic model of the optronic device is constituted of an ogive profile equipped with a small window and the tests are performed at Mach 3.7 with a very high Reynolds number. High speed interferograms are simultaneously recorded by a video camera and by a high speed camera (Cordin 350 Dynafax) at a high framing rate (20.000 images per second).

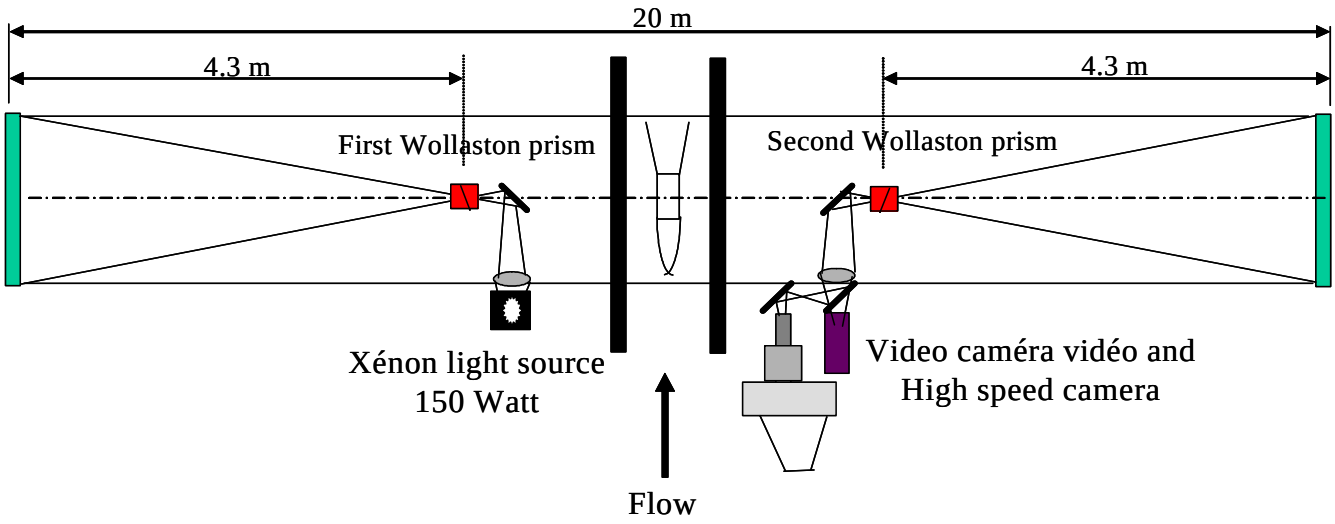

Fig.1. Differential interferometry implemented in S3MA wind tunnel of ONERA

2.2 Recorded interferograms and analysis

About 200 interferograms have been recorded per run and only a few of them are presented here. First, two types of Wollaston prisms have been used to observe the sensitivity of the same test configuration (Mach 3.7, high Re). Fig. 2 shows the obtained interferograms where the time exposure is 750 nanoseconds.

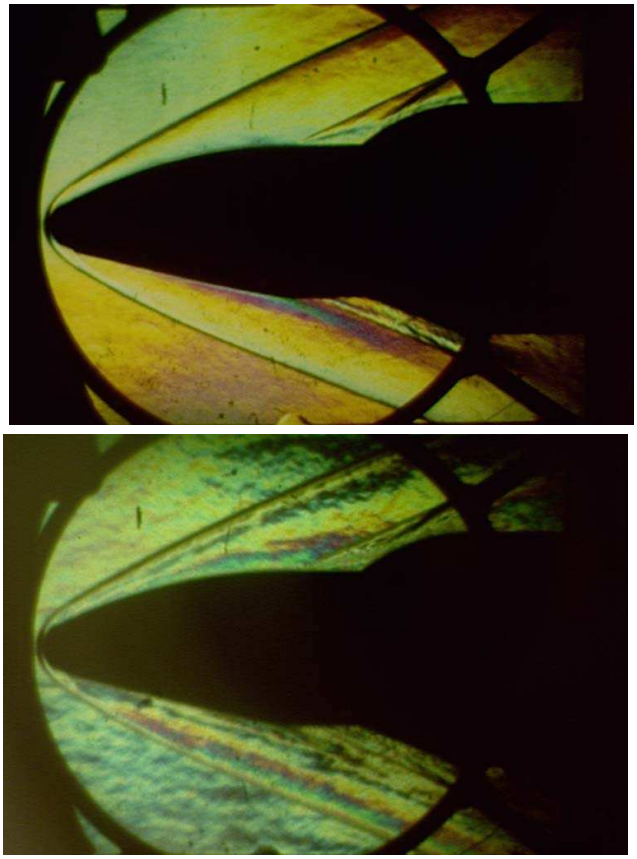

Fig.2. Instantaneous interferograms

First, it can be seen that a quasi uniform background color is obtained in front of the shock wave which makes easier the interferograms analysis. Since the interferograms are recorded with horizontal fringes, vertical gradients of the refractive index are detected and interferograms are analyzed assuming that the flow structure is axisymmetric. The optical path difference is determined by analysis of the colors in the upper and lower half planes. For that, a numerical model has been built from the optical interference laws to compute the optical path difference knowing the light intensity of interferences fringes [3]. Then, the optical thickness is obtained by integrating the optical path difference and the radial density distribution is computed using a deconvolution method. Fig. 3 shows the three steps of the interferogram analysis.

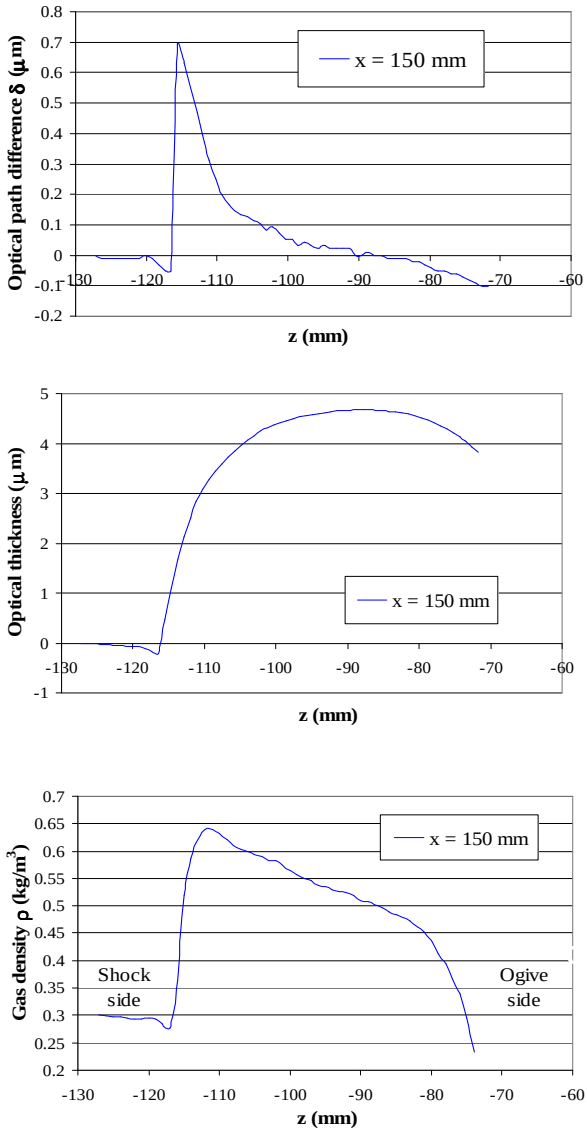

Fig.3. Steps of the interferogram analysis

3 Skin friction measurements

3.1 Principle and experimental setup

The interference fringes obtained under white light by a thin oil film have been used to measure the skin friction coefficient distribution

on the small window implemented on the lower surface of the ogive. The principle of this technique and the phenomenon modeling can be found in references [4, 5, 6] and the extension of the technique to color analysis is described in detail in reference [7]. In order to correctly depose the oil film, the model has been rotated by 45°. The xenon light source and the camera are located on the same side of the test section at an angle of incidence of θ_i as it can be seen in Fig. 4.

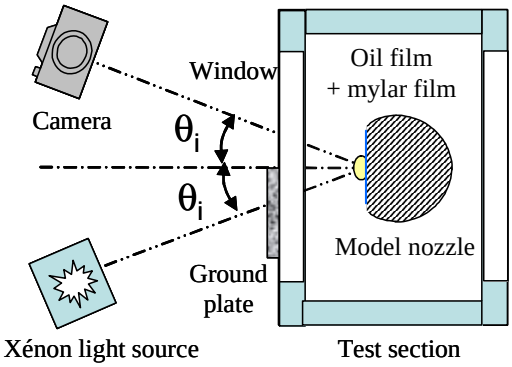

Fig.4.Setup of oil-film interferometry (OFI)

A Mylar film with a higher refractive index than the oil film is deposited on the model surface in order to increase the fringe contrast. Fig. 4 also shows a frosted glass which is placed just opposite to the test section on the side of the incident beam. This greatly improves the quality of the fringe images, because the frosted glass diffuses the light and turns the lamp into an extended source, which is the desired type of source for OFI. Then, oil drops have been deposited at different locations x on the model surface for two states of the boundary layer: x=56mm for the case of the natural transition and x=78mm for the case of the imposed transition. The oil viscosity used was 300 centistokes and t_0=0 was taken when the wind tunnel was running. The interference fringes have been photographed using a conventional film camera (f55mm at f11) at the rate of 24 frames per second.

3.2 Interferences analysis and results

Fig. 5 shows an example of interferences fringes obtained and its evolution in time. The model of the color luminous interferences generated by a white light source (continuous spectrum) shows that a color corresponds to an optical path difference δ [3]. Then, the oil-film thickness h versus δ is given by the following relation:

$$h = \delta / 2(n^2_{oil} - n^2_{air} \sin^2\theta_i)^{1/2} \qquad (1)$$

Assuming external pressure and stress gradients have no influence, the parietal stress τ_P can be expressed by:

$$\tau_P = 2(\rho_{oil} v_{oil} x'.n_{eq}) / \delta t \qquad (2)$$

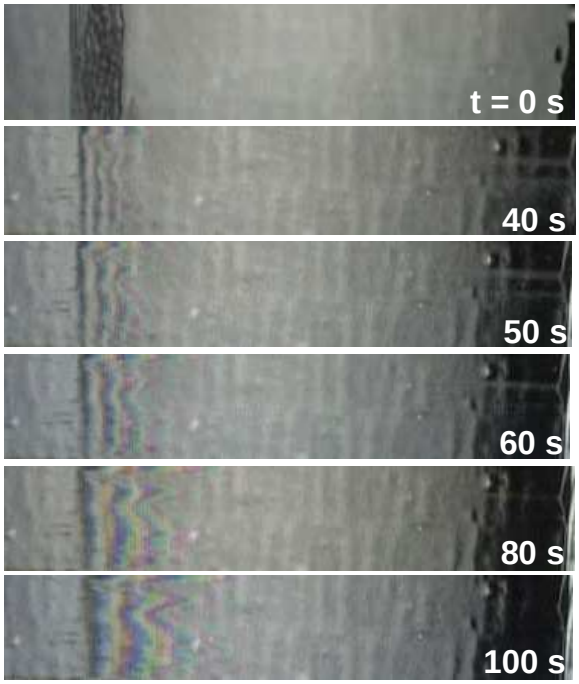

Fig.5 Evolution of interference in time

It can be seen that the fringe contrast is very good, which greatly facilitates analysis. The first three or four orders of interference in white light can even very clearly be seen, but the colors are no longer discernible beyond. The raw measurements of the optical path difference between interfering beams are plotted in the top graph of Fig. 6 versus the time. In this graph, the origin of the drop oil x' is identified in the first picture of Fig. 5. The curves vary almost linearly versus x', which allows a linear regression to be made for each time t, with

correlation coefficients close to 1. As regards Eq. (2), products h.t or δ.t must be constant for a given x' and for each analysis time. The next step of the analysis has consisted in evaluating the wind tunnel startup time t_0 in order to make constant the product δ.(t-t0). The second graph in Fig. 6 shows the variation of product δ.(t-t0) versus x' for t_0 = 18s.

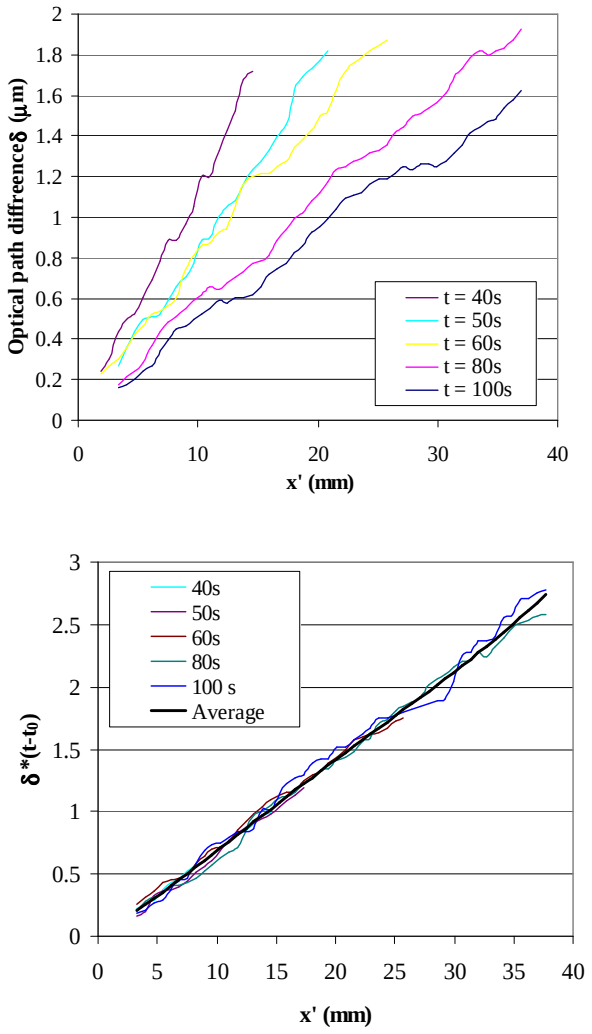

Fig.6. Determination of optical path difference and linear regression on the product δ.(t-t0)

4. Comparisons with RANS calculations

The elsA software developed at ONERA [8] solves the Navier-Stokes equations using a cell-centered finite-volume method. The upwind second order Roe scheme is used for the calculation of the numerical fluxes. The time integration is performed with a backward Euler scheme using an implicit LU method. Laminar or turbulent calculations can both be considered.

The half-model grid includes 4.200.000 nodes distributed in 12 structured blocs. It was built with the ICEM-CFD software. To compare with the experiments the numerical data is first interpolated in two additional grids located at the lower and upper sides of the model.

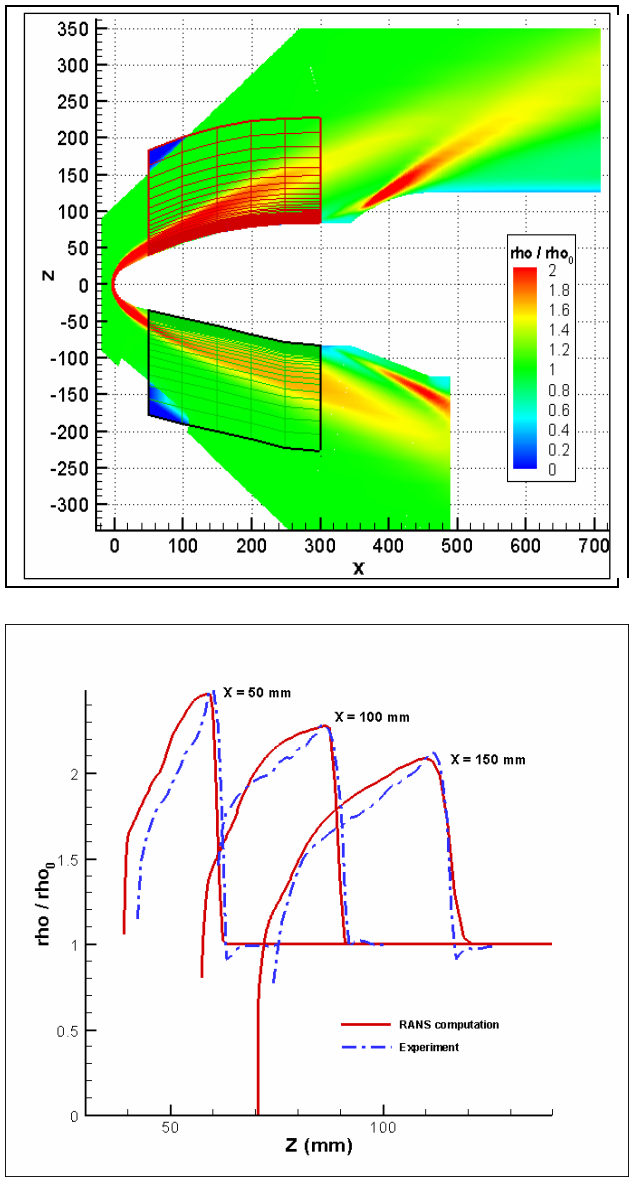

Fig.7 Mesh used for RANS computation and gas density radial distribution on upper surface

A comparison with the experiment is made around the ogive, at the upper side (small window located at the lower side) since the flow

can be considered axisymmetric in this region. Fig. 7 shows a good agreement between measured and calculated density profiles in three sections of the symmetry plane (x=50mm, 100mm and 150mm). The calculation is performed with the Spalart-Allmaras (SA) turbulence model from the nose.

For abscissa X > 150 mm the experimental results strongly differ from the RANS results. This is probably due to the fact that the flow axisymmetry assumption is no longer valid in this region.

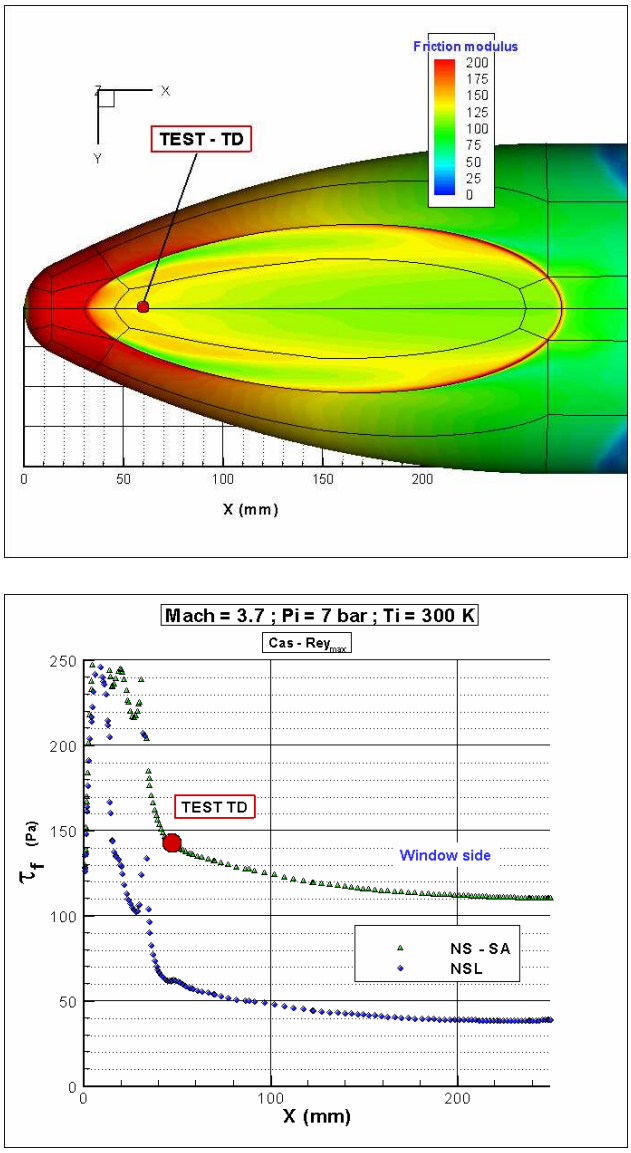

Fig.8. Comparison experimental-RANS computation of parietal stress

Figure 8 shows the friction modulus distributions calculated along the lower side of the model in the symmetry plane for both laminar and turbulent cases. One turbulent measurement point is also plotted (the transition is triggered 20mm downstream the nose of the ogive).

The location of the oil-film patch (red point in figure 8) is just beside the edge of the small window.

The measured stress is close to 150 Pascal which is close to the calculated value. One can find the list of the different parameters influencing the accuracy of the measurement in reference [7], such as oil viscosity, location of the oil-film origin, angle of incidence of the camera. One can estimate that the parietal stress is measured with an accuracy of 5.

Conclusion

Two new optical methods have been successfully tested in the very large S3MA wind tunnel of ONERA. First, a differential interferometric bench has been adapted and high speed interferograms obtained have allowed the analysis of several different configurations. The radial gas density distributions are in good agreement with the RANS results in the region where the flow can be considered axisymmetric. Concerning the oil-film skin-friction measurement, the technique has been tested in a supersonic flow (Mach 3.7). The phenomenon modeling, where the terms of gravity and pressure gradients are neglected, allows obtaining the parietal stress. Since the boundary layer transition is imposed, experimental results and NS-SA computation are very close.

References

[1] Gontier G. *Contribution à l'étude de l'interférométrie différentielle à biprisme de Wollaston.* Pub. Sci. et Tech. du Ministère de l'air, Paris, 1957.

[2] Françon M. and Sergent B. Compensateur biréfringent à grand champ. *Opto Acta*, pp 182-184, 1955.

[3] Desse J.M. Recording and processing of interferograms by spectral characterization of the interferometric setup. *Exp. In Fluids*, vol. 23, pp 265-271, 1997.

[4] Tanner, L.H., and Blows, L.G. A Study of Motion of Oil Films on Surfaces in Air Flow with Application

to the Measurement of Skin Friction, *Journal of Physics E*, Vol. 9, No. 3, pp. 194-202, 1976.

[5] Squire,, L.C. The Motion of a Thin Oil Sheet under the Steady Boundary Layer on a Body. *Journal of Fluid Mechanic*, Vol. 11, pp. 161-179, 1961.

[6] Zilliac, G.G. Further Developments of the Fringe-Imaging Skin Friction Technique. *Nasa Technical memorandum*, No. 1100425, December 1996.

[7] Desse J.M. Oil-film interferometry skin-friction measurement under white light, AIAA Journal, vol. 41, n° 12, pp. 2468-2477, 2003

[8] Cambier L. and Veuillot J.-P. Status of the elsA CFD Software for Flow Simulation and Multidisciplinary Applications, AIAA Paper 2008-664, Reno, Janvier 2008

Copyright Statement